

Enhancement of spin to charge conversion efficiency at the topological surface state by inserting normal metal spacer layer in the topological insulator based heterostructure

Sayani Pal,¹ Anuvab Nandi,¹ Shambhu G. Nath,¹ Pratap Kumar Pal,²
Kanav Sharma,¹ Subhadip Manna,¹ Anjan Barman,² and Chiranjib Mitra^{1,*}

¹*Department of Physical Sciences, Indian Institute of Science Education
and Research Kolkata, Mohanpur 741246, West Bengal, India*

²*Department of Condensed Matter and Materials Physics,*

S. N. Bose National Centre for Basic Sciences, Salt Lake, Kolkata 700106, India

(Dated: November 20, 2023)

We report efficient spin to charge conversion (SCC) in the topological insulator (TI) based heterostructure ($BiSbTe_{1.5}Se_{1.5}/Cu/Ni_{80}Fe_{20}$) by using spin-pumping technique where $BiSbTe_{1.5}Se_{1.5}$ is the TI and $Ni_{80}Fe_{20}$ is the ferromagnetic layer. The SCC, characterized by inverse Edelstein effect length (λ_{IEE}) in the TI material gets altered with an intervening Copper (Cu) layer and it depends on the interlayer thickness. The introduction of Cu layer at the interface of TI and ferromagnetic metal (FM) provides a new degree of freedom for tuning the SCC efficiency of the topological surface states. The significant enhancement of the measured spin-pumping voltage and the linewidth of ferromagnetic resonance (FMR) absorption spectra due to the insertion of Cu layer at the interface indicates a reduction in spin memory loss at the interface that resulted from the presence of exchange coupling between the surface states of TI and the local moments of ferromagnetic metal. The temperature dependence (from 8K to 300K) of the evaluated λ_{IEE} data for all the trilayer systems, TI/Cu/FM with different Cu thickness confirms the effect of exchange coupling between the TI and FM layer on the spin to charge conversion efficiency of the topological surface state.

Materials with efficient spin-charge interconversion (SCI) in the realm of Spintronics is gathering increasing attention due to their capacity to facilitate the development of energy-efficient spin-based devices. Enhanced SCI can be achieved by harnessing the spin orbit coupling (SOC) induced effect in different systems. Spin Hall SOC in heavy metals, Rashba SOC in two-dimensional electron gas (2DEG) at certain surfaces and interfaces and spin-momentum locked surface states in topological insulators (TI) yield substantial SCI capabilities. Recent experiments have observed remarkable spin-charge interconversion (SCI) in heterostructures based on TI [1–3]. One versatile method of SCI that stands out is the spin pumping experiment [23, 35, 37]. This process generates a spin current through the precession of magnetization in a ferromagnetic layer. The resulting spin current polarization aligns with the precession axis and induces a spin imbalance on the TI surface as the accumulated spin polarization diffuses into the TI. This imbalance, owing to the unique spin texture of TI state known as spin-momentum locking, leads to a spin accumulation and the creation of an electric field along the transverse direction via inverse Edelstein effect (IEE) as demonstrated in the Fig.1a. The parameter known as IEE length, λ_{IEE} involves the conversion of spin accumulation at the TI/FM interface into a transverse electric field in the TI and it quantifies the strength of spin to charge conversion (SCC) within the system. λ_{IEE} for the TI surface state can be expressed as $\lambda_{IEE} = j_c^{2D}/j_s^{3D} = v_F\tau$ where j_s^{3D} is the injected

spin current density from FM and j_c^{2D} is the generated charge current density in TI respectively. v_F is the Fermi velocity of the Dirac fermions and τ is the relaxation time of the non-equilibrium spin density distribution at the TI surface state [4]. IEE at the topological surface state (TSS) is found to be more efficient in SCI than the conventional inverse spin Hall effect in heavy metals[5–7]. However, the TI/FM interface may have significant effect on the SCI efficiency of the device in the following ways: i) spin density from Rashba-split 2DEGs at the TI/FM interface [10], originated from band bending [9] can negatively affect the SCI of the device; ii) presence of exchange coupling between TI surface state and FM can introduce spin memory loss at the interface [25] and, iii) material intermixing [17] at the interface of TI and FM can lead the formation of hybridization state and magnetic dead layer [8]. These deviations from an ideal TI/FM interface can play a critical role in suppressing the SCI efficiency. Thus for future TI-based spintronic devices we need a complete understanding of the interface effect on the efficiency of the devices.

In this paper, we demonstrate the spin-electricity conversion at the TI surface state and at the interface of TI with ferromagnetic and non-magnetic metals. To achieve this, we examined a specific heterostructure, $BiSbTe_{1.5}Se_{1.5}/Cu/Ni_{80}Fe_{20}$, by performing the ferromagnetic resonance (FMR) and spin-pumping measurements. We chose $BiSbTe_{1.5}Se_{1.5}$ as the 3D TI material where the surface state conduction dominates even at room temperature, thanks to the negligible bulk state contribution in conduction[11, 12]. We took Cu as the spacer layer between $BiSbTe_{1.5}Se_{1.5}$ (BSTS) and

* Corresponding author: chiranjib@iiserkol.ac.in

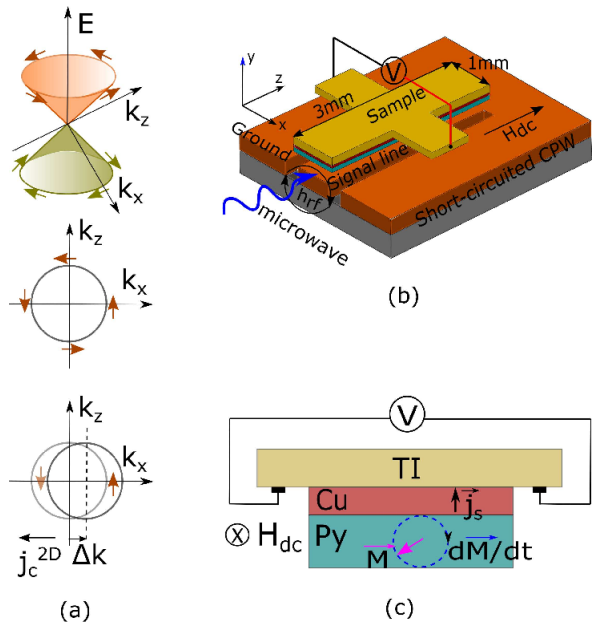


FIG. 1. Schematic illustration of the (a) concept of spin-to-charge conversion at TSS. Top panel: The energy dispersion relation of TSS with helical spin configurations of opposite chirality above and below the Dirac cone. Middle panel: spin configuration of the Fermi surface of TSS. Bottom panel: depicts the IEE in the device. The injected spin density from FM layer, j_s^{3D} with a specific polarity (here dark shaded orange arrow), accumulates at the TI surface state and creates an imbalance of spin population and generates a charge current, j_c^{2D} on the plane of surface state of TI; (b) experimental set-up for spin-pumping measurements on $BiSbTe_{1.5}Se_{1.5}/Cu(t)/Ni_{80}Fe_{20}$ heterostructure and (c) cross-section of the sample at the FMR resonance condition when magnetization, M precesses around the external dc magnetic field (H_{dc}) and due to the precession of magnetization (dM/dt), a spin current gets injected from the FM layer into the TI layer with spin-current density, j_s and spin polarization along the direction of the H_{dc} field.

$Ni_{80}Fe_{20}$ (Py) because Cu has long spin diffusion length and the Cu/Py interface has higher spin scattering asymmetry. The Cu/Py interface exhibit strong spin filtering due to weak majority-spin scattering and strong minority spin scattering at the interface [36].

We have prepared the heterostructure, $BiSbTe_{1.5}Se_{1.5}/Cu/Ni_{80}Fe_{20}$, with varying thicknesses of the copper layer (0.5 nm, 1.5 nm, and 3 nm). The thickness of the BSTS layer and the Py layer remained constant at 37 nm and 20 nm, respectively. Dimensions of the sample has been described in detail in the schematic diagram shown in Fig.1b. For clarity, we designated the different thicknesses of Cu as follows: Cu1 for 1.5 nm Cu and Cu2 for 3 nm Cu. The schematic diagram shown in Fig.1b illustrates the arrangement for FMR and spin pumping measurements. The sample has been placed on top of a coplanar waveguide having signal line width, $900 \mu m$ and characteristic impedance of 50Ω [15]. An external magnetic field, (H_{dc}) in

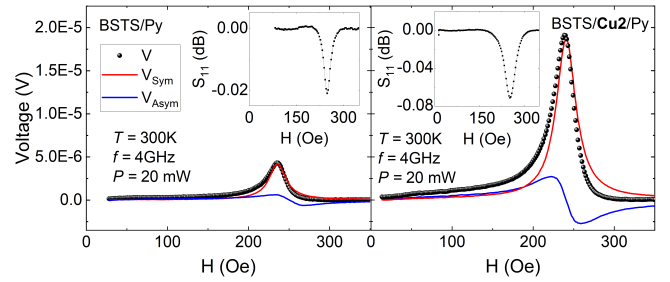


FIG. 2. Spin-pumping voltage (V) measured for the samples $BSTS/Py$ and $BSTS/Cu(3nm)/Py$ at room temperature where V_{Sym} and V_{Asym} represents the symmetric and anti-symmetric component of the measured voltage at microwave power (P) of 20mW. The figures in the inset presents the typical FMR spectra at room temperature at resonance frequency of 4GHz.

the plane of the sample and a microwave field (h_{rf}) of frequency $5GHz$, perpendicular to H_{dc} has been applied. The magnetization precession inside the FM layer at ferromagnetic resonance condition pumps spin angular momentum into the TI layer and it results in a spin accumulation at the TI surface state which in-turn develops into a transverse voltage across the TI in the microVolt range. The spins remain confined within the interface plane due to the two-dimensional nature of the topological surface state (TSS) and move perpendicular to the direction of spin polarization.

In Fig.2, the transverse voltage signal (V) as a function of external magnetic field (H) and the typical FMR resonance spectra (please refer to the inset figures) has been shown for $BSTS/Py$ and $BSTS/Cu(3nm)/Py$ respectively. The voltage measured between the two electrodes can be described by two components: the spin-pumping voltage signal that has the form of a symmetric Lorentz function, V_{Sym} and the voltage contribution from the possible anomalous Hall effect (AHE) and anisotropic magnetoresistance (AMR) of the magnetic layer (Py), V_{Asym} which has the form of antisymmetric Lorentz function[13, 14]. By fitting the measured voltage to the form $V = V_{Sym}(\Delta H^2/(\Delta H^2 + (H - H_{res})^2)) + V_{Asym}((\Delta H(H - H_{res}))/(\Delta H^2 + (H - H_{res})^2))$, the V_{Sym} component has been extracted for further evaluation of parameters useful for studying spin to charge conversion (SCC) at the TI surface state (TSS).

In Fig.3a, the microwave power response of V_{Sym} for $BSTS/Py$ and $BSTS/Cu2/Py$ has been shown at the excitation frequency of 4 GHz at room temperature and at low temperature respectively. The symmetric component of the measured voltage varies linearly with the microwave power for all the samples as can be seen from Fig.3b. The linearity suggests that the measured voltage is induced by the inverse Edelstein effect (IEE) as a result of spin pumping from the FM layer into the TI surface state[16–18]. We can observe from Fig.3b that the introduction of the Cu layer at the interface between the BSTS

and Py layer leads to a general rise in the value of V_{Sym} . Additionally, in Fig.3c, we can see that the trilayer device exhibits an enhancement in the damping coefficient (α) value compared to the single layer Py film and $BSTS/Py$ bilayer. It depicts the fact that the insertion of Cu layer definitely enhances the spin pumping efficiency in the device. We have calculated the effective spin mixing conductance, $g_{eff}^{\uparrow\downarrow}$ which is a material parameter that governs the transport of spin current into the adjacent NM layer from the FM layer and is proportional to the torque acting on the FM in the presence of spin accumulation in the NM layer [19, 20]. In Fig.4a, the variation of effective spin-mixing conductance (g_{eff}) with Cu thickness shows an increase in the g_{eff} value for $BSTS/Cu/Py$ samples compared to $BSTS/Py$ bilayer. g_{eff} was evaluated from the relation $g_{eff} = (2\sqrt{3}\pi M_{eff}\gamma d_{FM}(\Delta H_{bi} - \Delta H_{fm}))/g\mu_b\omega$ [23]. Given that g_{eff} takes into account the spin back flow into the FM layer and expresses the net transfer of spins from the FM, the variation of g_{eff} with t_{Cu} in Fig.4a validates the fact that spin transmission from Py layer into the adjacent non-magnetic layer has been enhanced by the insertion of Cu layer. Having known the g_{eff} , we have calculated the spin current density (j_s^0) injected from FM layer into the TI layer by using equation, $j_s^0 = (g_{eff}^{\uparrow\downarrow}\gamma^2\hbar^2[M_{eff}\gamma + \sqrt{(M_{eff})^2\gamma^2 + 4\omega^2}])/(8\pi\alpha^2[(M_{eff})^2\gamma^2 + 4\omega^2])$ [23]. The evaluated j_s^0 and the measured V_{Sym} value were used to calculate the inverse Edelstein effect length, $\lambda_{IEE} = j_C/j_s^0$ [24] where we have calculated j_C from the amplitude of the symmetrical Lorentz voltage, V_{Sym} by using the equation, $j_C = V_{Sym}/Rl$ where l is the length of the sample and R is the resistance of the sample measured using four probe method [22]. From Fig.4b, one can clearly see that at room temperature the λ_{IEE} value has been enhanced for trilayer samples compared to the $BSTS/Py$ bilayer and the change in Cu thickness tunes the λ_{IEE} . The enhancement of the λ_{IEE} for all the trilayer samples suggest a boosting of the net transfer of spin current into the TI layer by minimizing interfacial exchange coupling between the surface state of the TI and the local magnetic moments of the ferromagnetic (FM) material [17, 21] due to the insertion of the Cu layer in between the $BSTS$ and Py layer. For a complete understanding of the sensitivity of the λ_{IEE} value on t_{Cu} for the trilayer samples and to ensure the effect of any possible exchange coupling on the SCC efficiency (λ_{IEE}) of the device, one needs a low temperature measurement because the exchange interaction occurs between the surface state of TI (TSS) and the magnetic moment of FM and the TSS completely takes over the conduction when we reach low-temperature region.

In the proceeding section, we have tried to understand the specific role of TSS in spin-charge conversion. We conducted low temperature measurements on the following samples: $BSTS/Py$, $BSTS/Cu1(1.5\text{ nm})/Py$, and $BSTS/Cu2(3\text{ nm})/Py$ where the surface state of TIs dominate conductivity the most. Throughout the experi-

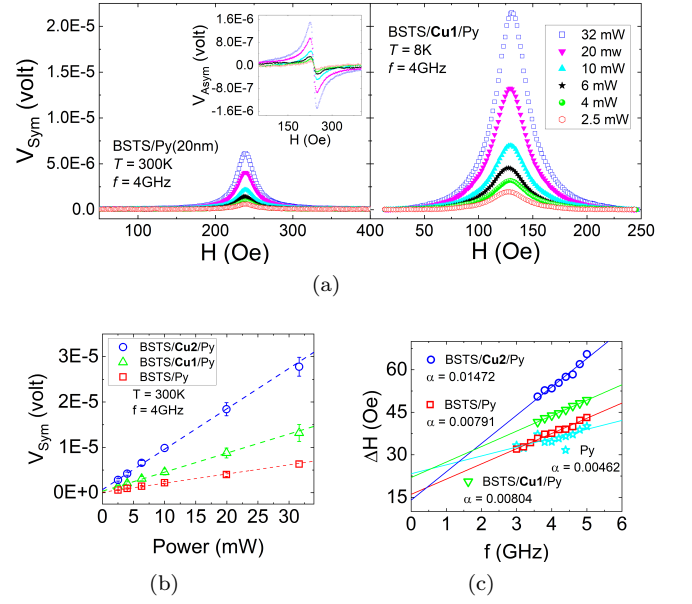


FIG. 3. (a) Measured spin-pumping voltage (V_{Sym}) of the samples, $BSTS/Py$ and $BSTS/Cu(1.5nm)/Py$ with varying microwave power at room temperature and at 8K respectively; The inset in the left figure shows V_{Asym} with varying power; (b) V_{Sym} varies linearly with the applied microwave power for all the heterostructure; (c) Linear fitting of FMR linewidth (ΔH) vs frequency (f) and the evaluated damping coefficient (α) values is shown for all the samples.

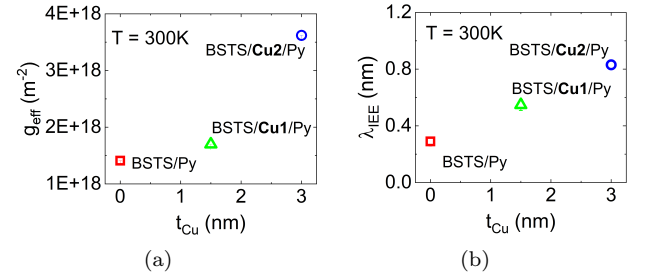


FIG. 4. Obtained (a) spin-mixing conductance (g_{eff}) and (b) spin to charge conversion length (λ_{IEE}) with varied Cu thickness at room temperature.

ment, we have used $BSTS$ thin films of thickness 37 nm as the TI material in the heterostructure. We have measured the temperature variation of resistance, R of the $BSTS$ sample which is shown in Fig. 5a. We have analysed the temperature dependence of conductance to estimate the contribution of surface states using a parallel resistor model following Singh *et al.* [12]. We find a 74% contribution of the TI surface state to the overall conductivity and a minimum leakage of spin current into the bulk of the 37 nm $BSTS$ film. We have measured V_{Sym} directly by probing the TI material. From Fig.5b one can see that the temperature variation of measured voltage for all the samples follow the same trend and it is concomitant with the resistance (R) vs. T plot shown

in Fig.5a. As the bulk resistivity increases with lowering temperature and surface conductivity becomes stronger, we are obtaining more voltage due to larger spin accumulation at the TSS. It again establishes the fact that the majority of the spin to charge conversion actually happens at the surface state of TI and not in the bulk of TI and the temperature dependence of voltage is primarily due to the inverse Edelstein effect (IEE) at the topological surface state. We have studied the temperature variation of FMR linewidth (ΔH) at a resonance frequency of 4 GHz as shown in Fig.5c. One can notice that the ΔH value shows an exponential increase for all the heterostructures once it reaches the temperature range where R saturates due to the maximum dominance of the surface state of TI. The ΔH enhancement proceeds monotonically with decrease in temperature and reaches the maximum value at the lowest temperature, 8 K for the sample with *Cu* spacer layer of thickness 3 nm. The g_{eff} vs. T shows a similar trend as that of ΔH as shown in the inset of Fig.5b. From the temperature variation data of both the parameters, g_{eff} and ΔH , we can state that lowering the temperature enhances the spin pumping from the FM layer into the adjacent non-magnetic layer. Now the question is whether the pumped spins accumulate directly in the TI surface state and get convert into a charge current via the Edelstein effect or significant losses due to spin memory loss are also involved in the process of spin to charge conversion at the interfaces. In the final section of our study, we investigated the temperature dependence of λ_{IEE} to understand the role of interface of TI/FM on the spin-charge conversion efficiency of the topological surface state. From the Fig.5d we can see that as temperature decreases from room temperature, the value of λ_{IEE} initially rises, but then decreases further as the temperature is lowered below a certain point. Spin memory loss at the interface of with the ferromagnetic metal (FM) could be a possible reason behind poor spin to charge conversion at TSS at low temperature. The theoretical model by V. P. Amin *et al.* [25] predicts that the interface transparency for spin transfer and the spin memory loss at interface depend on the interfacial SOC and interfacial exchange interaction respectively. Our previous study [32] with *BiSbTe*_{1.5}*Se*_{1.5}/*Ni*₈₀*Fe*₂₀ and other studies [33, 34] with other TI-based heterostructure suggest that TI/FM bilayers have high interfacial SOC and exchange coupling exists between the TI surface states and the local moments of FM. Spin memory loss that correlates the presence of exchange coupling strength can be significant when we lower the temperature below the point where the topological surface state completely takes over the conductivity. But one can suppress the exchange coupling by a proper separation of the TI and FM layer as can be seen for the sample with *Cu* thickness of 3 nm. For *BSTS/Cu2/Py* sample the λ_{IEE} value no longer decreases with temperature, indicates the fact that spin memory loss due to presence of exchange coupling got reduced and we achieved λ_{IEE} as large as 1.1 ± 0.03 nm at

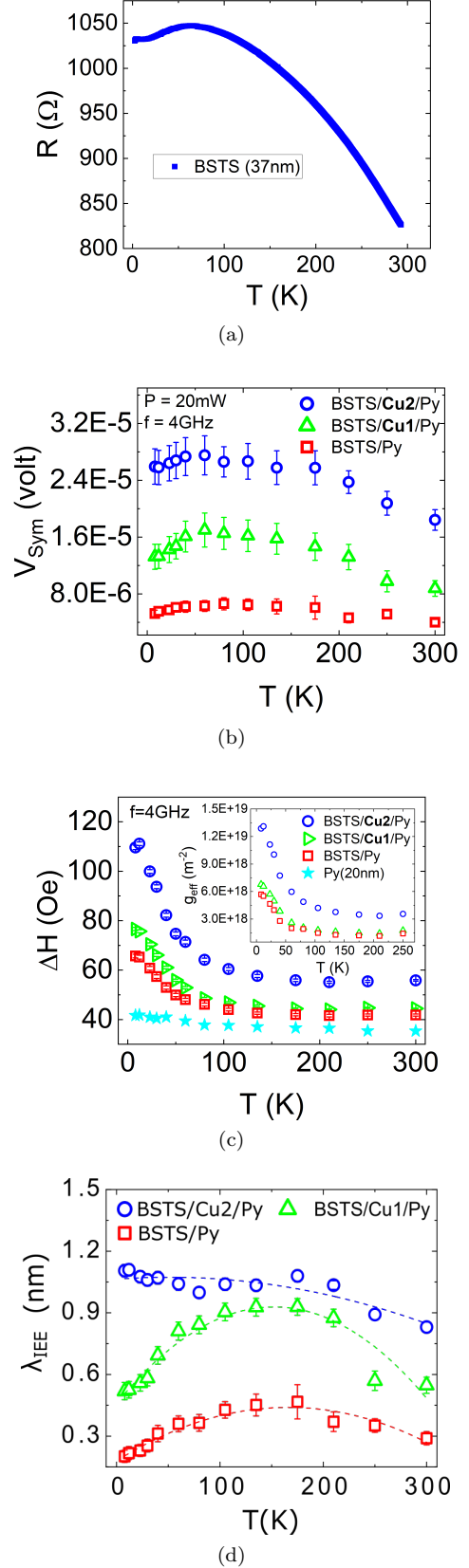


FIG. 5. Temperature dependence of (a) Resistance (R) for 37 nm *BiSbTe*_{1.5}*Se*_{1.5} thin film, (b) FMR spectra linewidth, ΔH (and spin-mixing conductance, g_{eff} in the inset), (c) Symmetric component of the measured voltage, V_{Sym} and (d) spin-to-charge conversion length (λ_{IEE}) for all the samples.

8 K and 0.8 ± 0.024 nm at room temperature. The λ_{IEE} value for our devices, especially for $BiSbTe_{1.5}Se_{1.5}/Cu(3\text{ nm})/Ni_{80}Fe_{20}$ are significantly higher in comparison to the other bilayer samples reported previously [1, 29–31] at lower temperatures as well as at room temperature. Thus to enhance the efficiency of TI-based heterostructures, a suitable choice of the interface layer is crucial. This choice serves to protect the unique spin texture of the topological surface state by reducing the exchange coupling between the TSS and the magnetic layer. In summary, we have observed a noteworthy improvement in the inverse Edelstein effect (IEE) length, which can be controlled by adjusting the thickness of the copper (Cu) layer positioned between the $BiSbTe_{1.5}Se_{1.5}$ and $Ni_{80}Fe_{20}$ layers. By conducting FMR and spin-pumping measurements on $BiSbTe_{1.5}Se_{1.5}/Cu/Ni_{80}Fe_{20}$, we determined a substantial λ_{IEE} value of 289 pm for $BiSbTe_{1.5}Se_{1.5}/Ni_{80}Fe_{20}$ structures. Upon introducing a Cu layer at the interface of the topological insulator (TI) and ferromagnetic (FM) layer ($BiSbTe_{1.5}Se_{1.5}/Cu(3\text{ nm})/Ni_{80}Fe_{20}$), we discovered that the λ_{IEE} can be enhanced further. Specifically, at low temperatures (8K), the insertion of Cu leads to a remarkably increased λ_{IEE} value of $(1.1 \pm 0.03)\text{ nm}$. Skillful

control over the Cu layer will enhance the efficiency of the device by reducing the spin memory loss at the interface that was caused by the presence of exchange interaction of the topological surface state and the local moments of ferromagnetic metal at the interface. The similarity in the temperature dependence of V_{Sym} with that of resistivity implies that the contribution to inverse Edelstein effect at low temperature is dominated by SCI from TSS. The topological protection of surface states increases the potential of the TI/FM bilayer for device application. In essence, our study offers promising ways for designing more efficient spin-charge conversion devices of the topological insulator based heterostructures by controlling the interface effects.

ACKNOWLEDGEMENTS

The authors sincerely acknowledge the Science and Engineering Research Board (SERB) (grant no: EMR/2016/007950), the Department of Science and Technology (grant no. DST/ICPS/Quest/2019/22), the DST-INSPIRE, the Council Of Scientific and Industrial Research(CSIR) and the University Grant Commission (UGC) of the Government of India for financial support.

-
- [1] Wang, X., Cheng, L., Zhu, D., Wu, Y., Chen, M., Wang, Y., Zhao, D., Boothroyd, C.B., Lam, Y.M., Zhu, J.X. and Battiatto, M., 2018. Ultrafast spin-to-charge conversion at the surface of topological insulator thin films. *Advanced Materials*, 30(52), p.1802356.
- [2] He, H., Tai, L., Wu, D., Wu, H., Razavi, A., Wong, K., Liu, Y. and Wang, K.L., 2021. Enhancement of spin-to-charge conversion efficiency in topological insulators by interface engineering. *APL Materials*, 9(7).
- [3] Wang, H., Kally, J., Lee, J.S., Liu, T., Chang, H., Hickey, D.R., Mkhoyan, K.A., Wu, M., Richardella, A. and Samarth, N., 2016. Surface-state-dominated spin-charge current conversion in topological-insulator-ferromagnetic-insulator heterostructures. *Physical review letters*, 117(7), p.076601.
- [4] Zhang, S. and Fert, A., 2016. Conversion between spin and charge currents with topological insulators. *Physical Review B*, 94(18), p.184423.
- [5] Mosendz, O., Pearson, J.E., Fradin, F.Y., Bauer, G.E.W., Bader, S.D. and Hoffmann, A., 2010. Quantifying spin Hall angles from spin pumping: Experiments and theory. *Physical review letters*, 104(4), p.046601.
- [6] Mosendz, O., Vlaminc, V., Pearson, J.E., Fradin, F.Y., Bauer, G.E.W., Bader, S.D. and Hoffmann, A., 2010. Detection and quantification of inverse spin Hall effect from spin pumping in permalloy/normal metal bilayers. *Physical Review B*, 82(21), p.214403.
- [7] Ando, K., Takahashi, S., Harii, K., Sasage, K., Ieda, J., Maekawa, S. and Saitoh, E., 2008. Electric manipulation of spin relaxation using the spin Hall effect. *Physical review letters*, 101(3), p.036601.
- [8] Wang, Y., Deorani, P., Banerjee, K., Koirala, N., Brahlek, M., Oh, S. and Yang, H., 2015. Topological surface states originated spin-orbit torques in Bi 2 Se 3. *Physical review letters*, 114(25), p.257202.
- [9] King, P.D.C., Hatch, R.C., Bianchi, M., Ovsyannikov, R., Lupulescu, C., Landolt, G., Slomski, B., Dil, J.H., Guan, D., Mi, J.L. and Rienks, E.D.L., 2011. Large tunable Rashba spin splitting of a two-dimensional electron gas in Bi 2 Se 3. *Physical review letters*, 107(9), p.096802.
- [10] Valla, T., Pan, Z.H., Gardner, D., Lee, Y.S. and Chu, S., 2012. Photoemission spectroscopy of magnetic and nonmagnetic impurities on the surface of the Bi 2 Se 3 topological insulator. *Physical Review Letters*, 108(11), p.117601.
- [11] Xu, Y., Miotkowski, I., Liu, C., Tian, J., Nam, H., Alidoust, N., Hu, J., Shih, C.K., Hasan, M.Z. and Chen, Y.P., 2014. Observation of topological surface state quantum Hall effect in an intrinsic three-dimensional topological insulator. *Nature Physics*, 10(12), pp.956-963.
- [12] Singh, S., Gopal, R.K., Sarkar, J., Pandey, A., Patel, B.G. and Mitra, C., 2017. Linear magnetoresistance and surface to bulk coupling in topological insulator thin films. *Journal of Physics: Condensed Matter*, 29(50), p.505601.
- [13] Mendes, J.B.S., Santos, O.A., Holanda, J., Loreto, R.P., De Araujo, C.I.L., Chang, C.Z., Moodera, J.S., Azevedo, A. and Rezende, S.M., 2017. Dirac-surface-state-dominated spin to charge current conversion in the topological insulator (Bi 0.22 Sb 0.78) 2 Te 3 films at room temperature. *Physical Review B*, 96(18), p.180415.
- [14] Su, S.H., Chuang, P.Y., Lee, J.C., Chong, C.W., Li, Y.W., Lin, Z.M., Chen, Y.C., Cheng, C.M. and Huang,

- J.C.A., 2021. Spin-to-Charge Conversion Manipulated by Fine-Tuning the Fermi Level of Topological Insulator (Bi_{1-x}Sb_x)₂Te₃. *ACS Applied Electronic Materials*, 3(7), pp.2988-2994.
- [15] Pal, S., Aon, S., Manna, S. and Mitra, C., 2022. A short-circuited coplanar waveguide for low-temperature single-port ferromagnetic resonance spectroscopy setup to probe the magnetic properties of ferromagnetic thin films. *Review of Scientific Instruments*, 93(8), p.083909.
- [16] Sun, R., Yang, S., Yang, X., Vetter, E., Sun, D., Li, N., Su, L., Li, Y., Li, Y., Gong, Z.Z. and Xie, Z.K., 2019. Large Tunable spin-to-charge conversion induced by hybrid Rashba and Dirac surface states in topological insulator heterostructures. *Nano Letters*, 19(7), pp.4420-4426.
- [17] Bonell, F., Goto, M., Sauthier, G., Sierra, J.F., Figueroa, A.I., Costache, M.V., Miwa, S., Suzuki, Y. and Valenzuela, S.O., 2020. Control of spin-orbit torques by interface engineering in topological insulator heterostructures. *Nano Letters*, 20(8), pp.5893-5899.
- [18] Shiomi, Y., Nomura, K., Kajiwara, Y., Eto, K., Novak, M., Segawa, K., Ando, Y. and Saitoh, E., 2014. Spin-electricity conversion induced by spin injection into topological insulators. *Physical review letters*, 113(19), p.196601.
- [19] Brataas, A., Nazarov, Y.V. and Bauer, G.E., 2000. Finite-element theory of transport in ferromagnet-normal metal systems. *Physical Review Letters*, 84(11), p.2481.
- [20] Brataas, A., Nazarov, Y.V. and Bauer, G.E., 2001. Spin-transport in multi-terminal normal metal-ferromagnet systems with non-collinear magnetizations. *The European Physical Journal B-Condensed Matter and Complex Systems*, 22(1), pp.99-110.
- [21] Kondou, K., Yoshimi, R., Tsukazaki, A., Fukuma, Y., Matsuno, J., Takahashi, K.S., Kawasaki, M., Tokura, Y. and Otani, Y., 2016. Fermi-level-dependent charge-to-spin current conversion by Dirac surface states of topological insulators. *Nature Physics*, 12(11), pp.1027-1031.
- [22] Sánchez, J.R., Vila, L., Desfonds, G., Gambarelli, S., Attané, J.P., De Teresa, J.M., Magén, C. and Fert, A., 2013. Spin-to-charge conversion using Rashba coupling at the interface between non-magnetic materials. *Nature communications*, 4(1), p.2944.
- [23] Jamali, Mahdi, Joon Sue Lee, Jong Seok Jeong, Farzad Mahfouzi, Yang Lv, Zhengyang Zhao, Branislav K. Nikolic, K. Andre Mkhoyan, Nitin Samarth, and Jian-Ping Wang. "Giant spin pumping and inverse spin Hall effect in the presence of surface and bulk spin orbit coupling of topological insulator Bi₂Se₃." *Nano letters* 15, no. 10 (2015): 7126-7132.
- [24] Rojas-Sánchez, J.C., Oyarzún, S., Fu, Y., Marty, A., Vergnaud, C., Gambarelli, S., Vila, L., Jamet, M., Ohtsubo, Y., Taleb Ibrahimi, A. and Le Fèvre, P., 2016. Spin to charge conversion at room temperature by spin pumping into a new type of topological insulator: α -Sn films. *Physical review letters*, 116(9), p.096602.
- [25] Amin, V.P. and Stiles, M.D., 2016. Spin transport at interfaces with spin-orbit coupling: Formalism. *Physical Review B*, 94(10), p.104419.
- [26] Greening, R.W., Smith, D.A., Lim, Y., Jiang, Z., Barber, J., Dail, S., Heremans, J.J. and Emori, S., 2020. Current-induced spin-orbit field in permalloy interfaced with ultrathin Ti and Cu. *Applied Physics Letters*, 116(5).
- [27] Wray, L.A., Xu, S., Neupane, M., Fedorov, A.V., Hor, Y.S., Cava, R.J. and Hasan, M.Z., 2013, July. Chemically gated electronic structure of a superconducting doped topological insulator system. In *Journal of Physics: Conference Series* (Vol. 449, No. 1, p. 012037). IOP Publishing. Marmolejo-Tejada, J.M., Dolui, K., Lazic, P., Chang, P.H.,
- [28] Smidstrup, S., Stradi, D., Stokbro, K. and Nikolic, B.K., 2017. Proximity band structure and spin textures on both sides of topological-insulator/ferromagnetic-metal interface and their charge transport probes. *Nano Letters*, 17(9), pp.5626-5633.
- [29] He H, Tai L, Wu D, Wu H, Razavi A, Wong K, Liu Y, Wang KL. Enhancement of spin-to-charge conversion efficiency in topological insulators by interface engineering. *APL Materials*. 2021 Jul 1;9(7).
- [30] Yamamoto, K.T., Shiomi, Y., Segawa, K., Ando, Y. and Saitoh, E., 2016. Universal scaling for the spin-electricity conversion on surface states of topological insulators. *Physical Review B*, 94(2), p.024404.
- [31] Sun, R., Yang, S., Yang, X., Vetter, E., Sun, D., Li, N., Su, L., Li, Y., Li, Y., Gong, Z.Z. and Xie, Z.K., 2019. Large Tunable spin-to-charge conversion induced by hybrid Rashba and Dirac surface states in topological insulator heterostructures. *Nano Letters*, 19(7), pp.4420-4426.
- [32] Pal, S., Aon, S., Manna, S., Nath, S.G., Sharma, K. and Mitra, C., 2023. Experimental investigation of the effect of topological insulator on the magnetization dynamics of ferromagnetic metal: *BiSbTe_{1.5}Se_{1.5}* and *Ni₈₀Fe₂₀* heterostructure. arXiv preprint arXiv:2303.07025.
- [33] Abdulahad, F.B., Lin, J.H., Liou, Y., Chiu, W.K., Chang, L.J., Kao, M.Y., Liang, J.Z., Hung, D.S. and Lee, S.F., 2015. Spin chemical potential bias induced surface current evidenced by spin pumping into the topological insulator Bi₂Te₃. *Physical Review B*, 92(24), p.241304.
- [34] Fanchiang, Y.T., Chen, K.H.M., Tseng, C.C., Chen, C.C., Cheng, C.K., Yang, S.R., Wu, C.N., Lee, S.F., Hong, M. and Kwo, J., 2018. Strongly exchange-coupled and surface-state-modulated magnetization dynamics in Bi₂Se₃/yttrium iron garnet heterostructures. *Nature communications*, 9(1), p.223.
- [35] Mukhopadhyay, S., Pal, P.K., Manna, S., Mitra, C. and Barman, A., 2023. All-optical observation of giant spin transparency at the topological insulator BiSbTe_{1.5}Se_{1.5}/Co₂₀Fe₆₀B₂₀ interface. *NPG Asia Materials*, 15(1), p.57.
- [36] Liu, R., Gupta, K., Yuan, Z. and Kelly, P.J., 2022. Calculating the spin memory loss at Cu—metal interfaces from first principles. *Physical Review B*, 106(1), p.014401.
- [37] Takahashi, S., 2014. Giant enhancement of spin pumping in the out-of-phase precession mode. *Applied Physics Letters*, 104(5)